Chapter 3

GIGAHERTZ FEMTOSECOND LASERS
The tools for precise optical frequency metrology

Albrecht Bartels
Time and Frequency Division, National Institute of Standards and Technology

Abstract: Femtosecond lasers with a repetition rate of approximately 1 GHz are commonly used frequency comb generators for precise optical frequency metrology. They are conveniently compact, yield unambiguous frequency readings with the help of a commercial wavemeter, and can yield greater heterodyne beat signals against a cw laser than systems with lower repetition rates. This chapter reviews the technology of oscillators based on Ti:sapphire and Cr:forsterite that operate at repetition rates of up to 3.5 GHz. Aside from a discussion of these "standard" lasers with a typical full-width-at-half-maximum (FWHM) bandwidth of 30 nm, one section is dedicated to the generation of a broadband continuum with a 1 GHz oscillator. This laser allows frequency measurements without additional spectral broadening and can be phase locked to a reference oscillator for uninterrupted periods exceeding one day.

Keywords: mode-locked lasers, optical atomic clocks, optical frequency metrology

1. INTRODUCTION

The first report of a femtosecond laser based on Ti:sapphire as the gain material was published in 1991 [1]. Since then a number of research groups have attempted to increase the repetition rate from 100 MHz to even higher values. In 1998, right before the dawn of optical frequency metrology with femtosecond laser combs, the oscillators by Ramaswamy et al. [2] and Stingl et al. [3] were conceptually the most intriguing for realizing higher repetition rates. Both researchers employed a new, more compact method for intracavity dispersion management, replacing the long prism sequences that had been part of every femtosecond laser until then. The prior configuration had prevented repetition rates higher than ≈300 MHz.
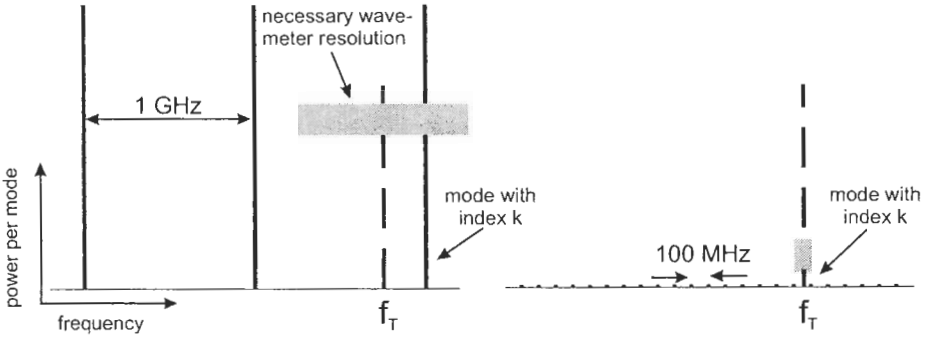
Figure 3-1. Illustration of the advantages for frequency metrology of the frequency comb emitted by a 1 GHz femtosecond laser (left) compared to that of a 100 MHz laser (right). The length of the two sets of comb teeth (solid vertical lines) scales with the power per mode. The lengths of the gray horizontal bars represent the necessary resolution for premeasurement of the frequency to be measured (f_T, indicated by the dashed line) to determine the index k of the mode against which f_T is beat.

In 1999 Udem et al. [4] demonstrated an optical frequency measurement with a femtosecond laser-based frequency comb for the first time. The comb was used to bridge the 18 THz wide gap between a calibrated reference frequency and the measured frequency f_T. Soon afterwards, Jones et al. [5] showed that a femtosecond laser can be "self-referenced." Self-referencing implies that both degrees of freedom of the optical frequency comb, the laser's repetition rate f_r and its carrier-envelope offset frequency f_0, are accessible and controllable. Because f_0 and f_r are electronically manageable microwave frequencies, the entire optical frequency comb with a multitude of components $v_n = f_0 + nf_r$ (where n is a large integer) in the hundreds of terahertz range can be directly linked to a cesium clock and subsequently used for absolute measurements of optical frequencies. Since then, many groups have successfully used femtosecond lasers for optical frequency measurements and to realize optical atomic clocks [6].

Even before these early experimental demonstrations of femtosecond laser-based optical frequency metrology, Reichert et al. [7] pointed out that repetition rates higher than the usually available 100 MHz would be greatly advantageous because they would yield a wider-spaced frequency comb. Typically in a frequency measurement, the result is given by $f_T = f_0 + kf_r + f_b$, where f_b is the frequency of the heterodyne beat between f_T and the neighboring frequency comb component with index k. While $f_0, f_r,$ and f_b can easily be measured, an unambiguous result for f_T requires determination of k via a premeasurement of f_T with a resolution of better than $\pm f_r/2$. In contrast to a 100 MHz system with a 1 GHz laser, this task is easily solved using a commercial wavemeter. (The best available wavemeter resolution within the

wavelength range of Ti:sapphire-based frequency combs is ≈100 MHz.) Also, with a cavity length of 30 cm, a 1 GHz oscillator is conveniently compact (commercially available models come in a ≈32×20×10 cm box) as compared to a 3 m long 100 MHz resonator. See Figure 3-1 for a comparison of the two systems.

A femtosecond laser with a 1 GHz repetition rate yields ≈100 times more usable optical power per comb component (mode) than does a 100 MHz laser. This additional power increases the signal-to-noise ratio of a heterodyne beat signal against a continuous-wave (cw) laser, which is used as a local oscillator to realize f_T, by the same amount. The factor of 100 is caused by two features of the femtosecond laser: First, the average output power of a well-designed Ti:sapphire laser is usually on the order of 25% of the absorbed pump power, regardless of the repetition rate. At a repetition rate 10 times higher, the average output power is distributed to one-tenth the number of modes, increasing the power per mode by a factor of 10. Second, the spectrally narrow output of a typical laser (FWHM ≈30–60 nm) needs to be broadened to span at least one octave via self-phase modulation (SPM) in a microstructure fiber [8] to allow self-referencing. However, nonlinear amplification of shot noise present on the input light limits the pulse energy that can be launched into a microstructure fiber and still attain usefully quiet output light [9, 10]. Above a threshold of ≈300 pJ of pulse energy, the excess noise on the fiber output grows exponentially. This behavior implies that a maximum average power of 300 mW in a 1 GHz system can be launched into a microstructure fiber. In comparison, only 30 mW can be sent into microstructure fiber in a 100 MHz system.

Some problems remain, related mainly to the long-term reliability of frequency metrology systems and their ease of use. A great improvement was achieved in 2004 with a 1 GHz laser that readily spans a broadband continuum and can be self-referenced without the use of microstructure fiber for uninterrupted periods in excess of one day. This oscillator will be addressed in the last section.

2.   HIGH-REPETITION-RATE RING OSCILLATORS

2.1   Design criteria and basic resonator layout

The repetition rate f_r of a passively mode-locked femtosecond laser is determined by the physical cavity length L and the round-trip-averaged group velocity $\bar{v}_g$:

$$f_r = \frac{\bar{v}_g}{L}.$$ (1)

Thus, increasing the repetition rate means shrinking the cavity length. The realization of gigahertz repetition rates for Ti:sapphire femtosecond lasers has been straightforward. A few simple specific design criteria now exist. They can be discussed in the context of a steady-state duration τ of a pulse circulating in a cavity in which only SPM, provided by the nonlinear refractive index $n_2 \approx 3\times10^{-16}\text{m}^2/\text{W}$ of the Ti:sapphire gain crystal, and negative group-delay dispersion (GDD), designated as D_2, shape the pulse (see, for example, Reference [11]). This limit applies in good approximation to all Kerr-lens–mode-locked femtosecond lasers as long as higher-order dispersion is negligible:

$$\tau = 4\ln\left(1 + \sqrt{2}\right)\frac{|D_2|\lambda w_0^2}{d\, n_2 E_P},$$ (2)

where λ is the carrier wavelength, w_0 is the waist radius inside the laser crystal, d the length of the crystal, and E_P the pulse energy.

When shrinking a 100 MHz cavity to yield a 1 GHz repetition rate, the pulse energy E_P is reduced by a factor of 10 (assuming constant average power). This results in a steady-state pulse duration 10 times longer. The combination of lower pulse energy and greater pulse duration reduces the peak by a factor of 100. This alone does not present a fundamental problem for achieving higher repetition rates. However, in practice Kerr-lens mode locking (KLM) is required to maintain stable pulsed operation over cw operation. A Kerr lens is induced by a high-intensity Gaussian beam profile in the Ti:sapphire crystal via its nonlinear refractive index. To achieve KLM, the cavity is arranged in a way that the Kerr lens modulates the net gain or loss of the cavity for a pulsed beam. Either it reduces the net cavity losses by increasing the transmission through a hard aperture (e.g., a slit) at an appropriate position in the resonator (hard-aperture KLM), or it increases the net gain by increasing the overlap with the finite gain volume inside the crystal (soft-aperture KLM). KLM gets more efficient with higher peak intensity. (High pulse energies and short pulse widths in the cavity are essential.) Thus the reduction of peak power due to the increased repetition rate must be compensated for. This is accomplished by reducing the amount of output coupling with respect to a 100 MHz oscillator (from $\approx$10% to $\approx$1%) and shrinking the waist radius w_0 inside the gain crystal by tighter focusing.

The second major concern is the achievement of negative net-GDD in the cavity. The standard method of employing a four-prism sequence (or a

double-passed, two-prism sequence) fails for high repetition rates because even with highly dispersive materials, an apex distance of ≈30 cm per prism pair is required [12]. This requirement sets an upper limit of ≈300 MHz on the repetition rate. An elegant way to replace a prism sequence is by using negative dispersion mirrors that reflect light with longer wavelengths from a deeper region in the coating than light with shorter wavelengths. A variety of structures has been developed, of which only Gires-Tournois interferometer (GTI) mirrors and chirped mirrors are used here [13].
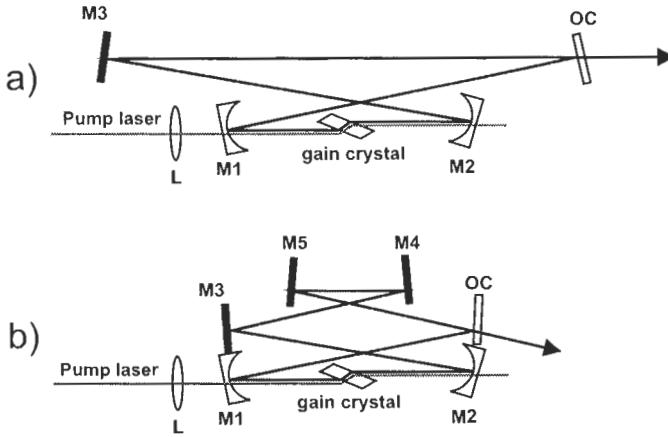

Figure 3-2. (a) Four-mirror cavity with the gain crystal enclosed by focusing mirrors M1 and M2. The flat mirror M3 and the output coupler (OC) form the collimated part of the cavity. The pump light enters the crystal through lens L and M1. (b) Equivalent to (a) but with extra folding using flat mirrors M4 and M5.

The ring oscillators shown in Figure 3-2 are the basis for all lasers presented here. A ring configuration has been chosen for geometrical reasons. With a given number of components, it allows a higher repetition rate than a linear cavity. Also, ring cavities are less sensitive to back-reflections. In the following sections, the cavities will be discussed in detail along with actually realized lasers.

As with all Kerr-lens–mode-locked femtosecond lasers, these oscillators need an initial perturbation, such as tapping a mirror mount, to generate an intracavity power fluctuation that builds up to a stable circulating femtosecond pulse. As opposed to cw operation, which is bidirectional, mode-locked operation is unidirectional and starts in a random direction [14].

2.2 Standard Ti:sapphire lasers for 0.3–3.5 GHz repetition rate

The four-mirror cavity, as shown in Figure 3-2(a), is usually employed to achieve the highest repetition rates because it can be made the most compact. The cavity contains a Ti:sapphire crystal of length d=1.5 mm (absorption coefficient α=5 cm^{-1}) that is pumped with a frequency-doubled Nd:YVO$_4$ laser at 532 nm through lens L with f_L = 30 mm. The crystal is placed at Brewster's angle between mirrors M1 and M2. The pump beam radius inside the crystal is ≈10 μm. Mirrors M1 and M2 have a focal length of 15 mm, leading to a calculated waist radius of the resonator mode inside the crystal between 8 and 20 μm for repetition rates ranging from 0.5 to 3.5 GHz. The angles at which the intracavity beam is reflected off M1 and M2 are set such that the cavity is astigmatically compensated [15]. The crystal introduces a GDD of ≈87 fs^2 at 800 nm wavelength. Chirped mirrors with a GDD of ≈ -45 fs^2 at 800 nm are used for M1–M3 to achieve a net GDD of ≈ -48 fs^2 (the GDD of the OC is negligible). The output coupler has a reflectance of 98%, and the cavity length is set to yield a repetition rate of 2 GHz.

This laser is operated at pump powers between 1.8 and 5.5 W. Figure 3-3 shows output power as a function of pump power with a rather low slope efficiency of 13.6%. The low efficiency is due to the short gain crystal, whose length is limited by the constraint to achieve a negative net GDD. However, if the absorbed pump power is considered, the slope efficiency rises to 25.8%.

Figure 3-4(a) shows a measured autocorrelation trace of the laser output when operating at 5.5 W pump power after compensation of extracavity dispersion by multiple reflections off a pair of chirped mirrors. The envelope of a 24 fs long pulse, assuming a sech$^2(t)$ intensity profile, is fitted to the trace, showing good agreement. Figure 3-4(b) shows the corresponding output spectrum with a FWHM of 32 nm. The time-bandwidth product of 0.35 deviates slightly from the ideal of 0.315. The inset of Figure 3-4(a) shows the pulse duration of the same laser operated at different intracavity pulse energies. (Variation of the pulse energy was attained by changing the pump power.) The theoretical pulse durations as a function of pulse energy, as in Equation (2), are also plotted in the inset and agree well with the experiment. (w_0 was calculated using ABCD matrices to generate the theoretical curve.) The agreement between theory and experiment confirms that SPM and GDD dominantly shape the pulses in this laser; thus, pulse width and bandwidth can be easily and well controlled.
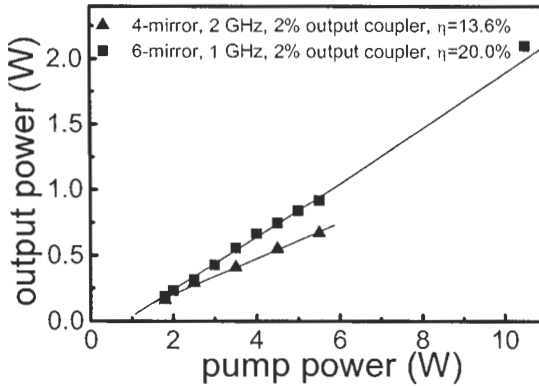
Figure 3-3. Laser output power as a function of incident pump power for the four-mirror (triangles) and six-mirror (squares) lasers described in the text. The solid lines are linear fits to the datasets.

Attempts to further shorten the pulse duration were undertaken by reducing $|D_2|$. We found a limit at 14 fs (at a spectral bandwidth of 70 nm FWHM) due to higher-order terms in the intracavity dispersion.
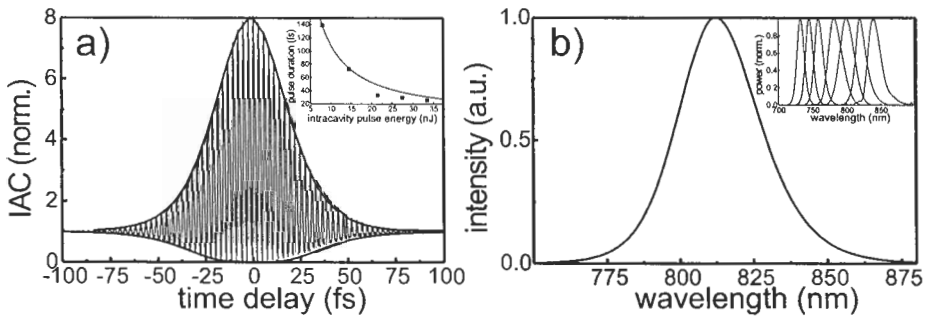

Figure 3-4. (a) Interferometric autocorrelation trace of the pulses from the four-mirror laser at 5.5 W pump power. Inset: Pulse duration as a function of intracavity pulse energy (squares) and theoretical values according to Equation (2). (b) Corresponding output spectrum. Inset: Series of output spectra of a continuously tunable version of the six-mirror cavity [16].

Often neglected in scientific papers, but important for real-world applications, is the beam quality of a femtosecond laser. Figure 3-5(a) shows a beam profile of the four-mirror cavity recorded at the focus after focusing the laser output with a lens of 200 mm focal length. It shows no noticeable deviation from circular symmetry. Figure 3-5(b) shows a cross section

through the beam profile with a fitted Gaussian, again with no noticeable deviation from ideal. A measurement of the M^2-factor has been performed, yielding values of 1.1 for both tangential and saggital planes. (See Reference [17] for a definition of M^2.) The excellent beam quality is attributed to the fact that spatially dispersive elements are absent in the cavity.

With the four-mirror cavity, repetition rates between 1 GHz and 3.5 GHz were attained. The upper limit was set by geometrical constraints, i.e., it has not been possible to move the components closer together. It is anticipated that even higher repetition rates of up to 10 GHz are feasible by minimizing mechanical components and further reducing the focal lengths of M1 and M2. The disadvantage of this cavity is that the short-gain crystal results in a relatively low output power.
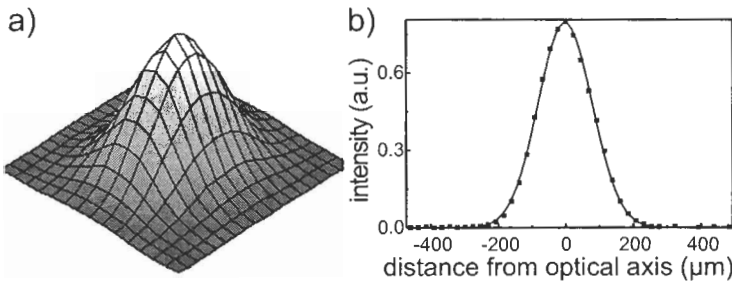

Figure 3-5. (a) Mode profile of a four-mirror laser at the focus of a 200 mm lens. (b) Cross section (squares) through the profile shown in (a) and fit with a Gaussian (solid line).

Folding with two additional negative dispersion mirrors in the cavity as in the six-mirror configuration shown in Figure 3-2(b) allows one to use a longer Ti:sapphire crystal, achieve more gain, and, at the same time, ensure a negative net GDD in the cavity. This approach is favored when higher output powers and moderate repetition rates are required. The oscillator depicted in Figure 3-2(b) has a crystal of length d = 2.5 mm and an absorption α = 5 cm^{-1}. It employs the same chirped mirrors that were used for the four-mirror cavity in positions of M1–M5 and has a repetition rate of 1 GHz. The net cavity GDD in this case is -80 fs^2. With a 2% output coupler, the output power as a function of incident pump power is shown in Figure 3-3. The slope efficiency is 20%; with respect to the absorbed pump power, it is 28%, comparable to that of the four-mirror laser. At the highest available pump power of 10.5 W, a remarkably high output power of 2.1 W is attained.

With respect to output spectra, pulse duration, and beam quality, the six-mirror cavity performs equivalently to the four-mirror cavity. It has been realized at repetition rates between 300 MHz and 2 GHz.

The two oscillators described in this section are widely used frequency comb generators for optical frequency metrology. They are commonly operated between 0.8 GHz and 1 GHz. This range has proven to be the best compromise between high-repetition rate and sufficient pulse energy to generate an octave-spanning spectrum in common microstructure fibers. (See e.g., Reference [18] for a typical octave-spanning spectrum from a 1 GHz four-mirror laser and a microstructure fiber.)

The six-mirror cavity has also been realized in a wavelength-tunable modification at a repetition rate of 1 GHz [16]. A half-Brewster prism was used to introduce spatial dispersion into the resonator with the effect that horizontally tilting a cavity mirror allowed continuous tunability from 733 to 850 nm with pulse durations of ≈40 fs. A series of output spectra is shown in the inset of Figure 3-4(b).

2.3   Cr:forsterite oscillator at 433 MHz — extension to telecommunication wavelengths

It is a logical step to extend the concept that has successfully been used with Ti:sapphire to gain media that operate at longer wavelengths. One reason is to obtain access to the telecommunication bands and thus be able to calibrate and characterize system components, such as wavelength references or wavelength-division multiplexing filters, in that region. A second goal is to generate a mode-locked spectrum that is adjacent to and that can be phase coherently combined with the output spectrum of a Ti:sapphire laser (specifically the one described in the next section) to generate an extraordinarily broad "superfrequency comb." The gain material that is best suited for both tasks is Cr:forsterite, which has a gain spectrum extending from wavelengths of ≈1150 to 1350 nm.

A femtosecond laser with Cr:forsterite was realized at a repetition rate of 433 MHz in the six-mirror configuration [see Figure 3-2(b)] [19]. The 10 mm gain crystal with an absorption coefficient of $\alpha=1.1$ cm^{-1} at 1075 nm is significantly longer than in the Ti:sapphire lasers to allow for sufficient pump light absorption. The crystal is pumped with 10 W from an Yb:glass fiber laser emitting at 1075 nm through a lens with $f_L = 40$ mm. The crystal is cooled to 0° C to increase the gain and to reduce problems with thermal lensing. (Cr:forsterite has a thermal conductivity ≈5 times lower than Ti:sapphire.) The focal lengths of mirrors M1 and M2 are 25 mm; they are longer than what has been used for the Ti:sapphire lasers to better match the confocal length of the cavity mode to the length of the gain crystal. With chirped mirrors at positions M1–M3, a GTI mirror at M4, a low-dispersive high reflector at M5, and the GDD of the gain crystal of 185 fs^2 [20], the net GDD is ≈ -260 fs^2. A 1.5% transmission output coupler at 1280 nm is used.

The mode-locked output power of this laser is 620 mW. A spectrum of the output pulses is shown in Figure 3-6. The spectral bandwidth is 59 nm centered around 1280 nm. The pulse duration of 30 fs was determined with an intensity autocorrelation measurement.

Alignment of this laser for stable mode locking is more difficult than for Ti:sapphire lasers. Ti:sapphire lasers consistently mode lock at the inner edge of the cavity's stability range, as expected from modeling KLM. This systematic guideline for finding mode-locked operation does not work in Cr:forsterite because of thermal lensing. However, once a working point has been found, the laser's operation is reliable and reproducible. Mode-locked operation has been observed uninterrupted for up to seven days.
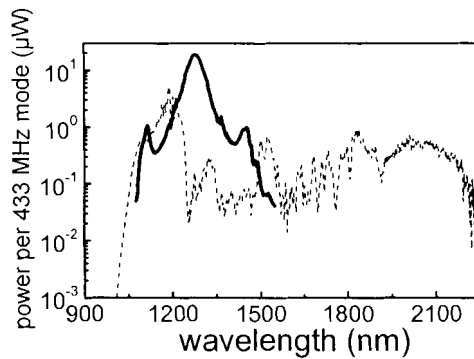

Figure 3-6. Output spectrum of the Cr:forsterite laser (solid line) and spectrum after broadening in a highly nonlinear Ge-doped silica fiber (HNLF) (dashed line).

The output from this laser was successfully broadened via SPM in highly nonlinear Ge-doped silica fiber (HNLF) to form a frequency comb that spans more than one octave [19, 21], as shown in Figure 3-6. This frequency comb has been referenced to the National Institute of Standards and Technology's (NIST's) Ca optical frequency standard and a cesium atomic clock. Its utility for optical frequency measurements was demonstrated by Corwin et al. [22] who used the broadened Cr:forsterite comb for the characterization of telecommunication-band frequency standards.

The creation of a phase-coherent superfrequency comb, ranging from wavelengths of 570 to 1450 nm, was demonstrated by actively linking the output of the Cr:forsterite laser, described above, and a broadband Ti:sapphire laser described in the next section [23].

3.   BROADBAND TI:SAPPHIRE OSCILLATOR

A new type of extremely broadband femtosecond laser has been realized with a slight modification of the four-mirror cavity described earlier [see Figure 3-2(a)]. The modified cavity has a convex mirror with a radius of curvature of 1 m at the position of M3. M1, M2, and M3 are chirped mirrors. The output coupler has a transmission of 2% at 800 nm. The net intracavity dispersion of the resonator, including air and the Ti:sapphire crystal ($d = 2.0$ mm), and the mirror reflectivities are shown in Figure 3-7. The net GDD at 800 nm is $\approx$ -20 fs^2. When the cavity is operated close to the inner edge of its stability range, continuous translation of mirror M2 towards M1 results in bidirectional mode locking and stages of stable and chaotic multipulsing in two directions and in one direction until a state with a single stable pulse circulating unidirectionally in the cavity is reached. At a pump power of 10.5 W, the mode-locked output power is $\approx$1 W. The cavity length is adjusted to yield a 1 GHz repetition rate.
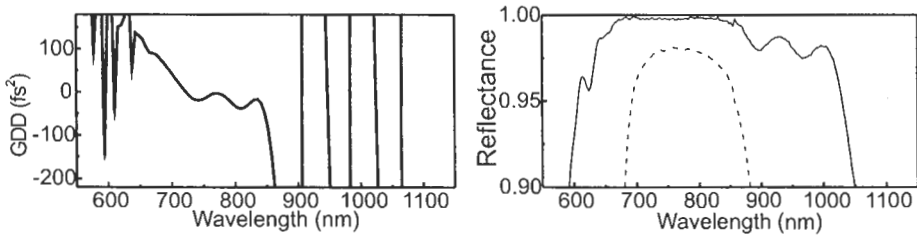

Figure 3-7. Left panel: Net cavity group-delay dispersion (GDD) of the broadband laser. Right panel: Reflectance of the chirped mirrors (solid line) and the output coupler (dashed line).

The output spectrum of the laser is shown in Figure 3-8. It spans from 570 to 1100 nm at a power level of 1 nW per 1 GHz frequency mode. (1 nW per mode is the power typically required to measure a beat note against a milliwatt-scale cw laser with sufficient signal-to-noise ratio for a frequency measurement.) The spectrum has pronounced maxima at 670 nm, 845 nm, 900 nm, and 927 nm. The peak around 670 nm can be isolated by a double reflection off a pair of 657 nm high reflectors, leading to the spectrum shown in the inset of Figure 3-8(b). It contains 450 mW of average power.

The duration of the output pulses has only been roughly characterized by using an intensity autocorrelation measurement. Assuming a temporal sech^2 shape, it is 11 fs when the nonlinear crystal is angle-tuned to optimally phase match the central part of the spectrum. The peak around 670 nm yields bandwidth-limited pulses of 33 fs after isolation from the longer-wavelength part of the spectrum.
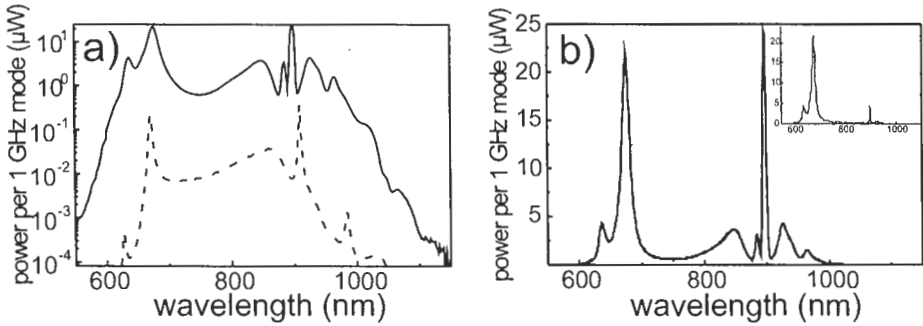
Figure 3-8. (a) Output spectrum of the broadband laser on a logarithmic scale (solid line). At a level of 1 nW per 1 GHz mode, it extends from 570 to 1100 nm. The dashed line shows a simulated spectrum, offset by 20 dB for clarity. (b) Output spectrum of the broadband laser on a linear scale. Inset: spectrum after reflection off a pair of 657 nm high reflectors.

3.1 How does it work?

The performance of this laser is extraordinary in a number of respects: First, when mode locking is stopped (e.g., by briefly intersecting the pump beam) and the laser falls back into cw operation, the output power drops by more than an order of magnitude to about 60 mW. Assuming that a Kerr-lens-based effective saturable absorber is responsible for this behavior, a simple rate equation model leads to the conclusion that ≈30% saturable absorption is required to explain this drop. This high saturable absorption contrasts with what is usually observed for standard Ti:sapphire femtosecond lasers, which have an effective saturable absorption of ≈1–2%. Second, considering the fact that Ti:sapphire has no gain below 690 nm, the 450 mW of power contained in the peak around 670 nm is very remarkable and indicates that this strong component is generated during only a few round trips through the cavity. Finally, assuming that SPM and GDD dominate pulse shaping, mode locking of the laser at such extreme bandwidth should not be possible. The strong GDD modulation and the positive values outside a band ranging from 700 to 850 nm should quickly spread the pulse and prevent mode locking (see Figure 3-7 for the net intracavity dispersion).

To get an idea of how this laser functions, it is helpful to review the two practical routes towards shorter pulses and broader spectra in a femtosecond laser. One approach is to engineer the dispersion inside the resonator in a way that short pulses with extremely broad spectra do not spread in time during a cavity round trip. This involves careful design of mirrors to have negative GDD over the desired large bandwidth and compensate for the positive-gain crystal dispersion with a low net-higher-order dispersion. This

approach has been taken with great success by Ell et al. [24]. Their carefully engineered intracavity dispersion is capable of generating spectra exceeding one octave with 5 fs pulses at a repetition rate of 64 MHz. In our case, however, because of the narrow bandwidth of the chirped mirrors, both with respect to their dispersive and reflective properties, this limit is inapplicable. Alternatively, one can allow higher-order dispersion in the resonator but, at the same time, ensure that the leading and trailing edges of the temporally spreading spectrum are sufficiently suppressed, such that only a short pulse remains stable in the cavity. This effect can be attained by employing an effective fast saturable absorber. In the case of our Ti:sapphire lasers, this effective saturable absorber is provided by a soft aperture KLM (see Section 2.1). While this effect is actually a self-gain modulation, it can theoretically be treated as an equivalent fast saturable absorber. These effects are more generally referred to as self-amplitude modulation (SAM).

There are strong indications that the broadband laser described above operates in the limit of an increased SAM. The strongest support for this idea is the experimental observation that the mode-locked output power and the continuous output power of the laser differ by more than an order of magnitude. This difference indicates that the Kerr-lens-induced effective saturable absorber has a saturable absorption of approximately 30%. Theoretical calculations of the change in beam waist diameter inside the gain medium (i.e., the soft-aperture Kerr-lens effect) show that replacing flat mirror M3 with a slightly convex mirror (in our case with a radius of curvature of 1 m) can increase the SAM of pulses circulating in the ring cavity [25]. While the theory applied to calculate this effect is valid only at power levels of about a factor of four below the power at which our oscillator operates, it still has provided a clue to understanding this new type of femtosecond oscillator.

A full theory explaining why the convex mirror leads to a stronger effective saturable absorber does not yet exist. However, modeling the resonator with a split-step Fourier simulation allows us to understand why this laser functions. The model includes the Ti:sapphire gain spectrum and dispersion, all reflective amplitude and phase properties of the cavity mirrors, SPM, and a fast saturable absorber (of the same type as used by Chen et al. [26]). The dashed curve in Figure 3-9 shows a simulation of a cavity with the same mirrors as the broadband laser cavity but with a shorter crystal (d = 1.5 mm) and a saturable absorption of $q_{sat.}$ = 2%. Its net GDD at 800 nm is -45 fs^2. It represents a standard laser with a relatively narrow spectrum of 45 nm bandwidth. An attempt to get shorter pulses from this laser by increasing the net cavity GDD to $\approx$ -20 fs^2 by using a longer crystal (d = 2.0 mm) fails because the simulation does not yield a stable solution anymore. Higher-order dispersion spreads the seed pulse and randomizes its

phase. However, when $q_{sat.}$ is increased to 30% for the $d = 2$ mm configuration, the model again delivers a stable solution, shown as the solid line in Figure 3-9. The solution corresponds to the new broadband laser where, despite dominant higher-order dispersion, a stable mode-locked solution is obtained because of the pulse-cleaning effect of the enhanced SAM. This simulation agrees very well with the experimental spectrum in its main features, which include the pronounced peaks at $\approx$670 nm and $\approx$900 nm, the asymmetric central contribution around 835 nm, and the spectrum's approximate width [see Figure 3-8(a)].
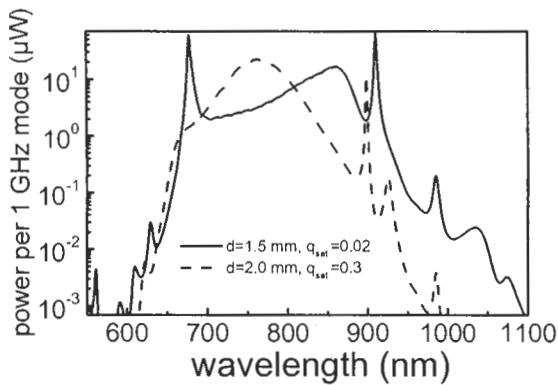

Figure 3-9. Modeled output spectra of a standard laser ($d = 1.5$ mm, $q_{sat.} = 0.02$) and a broadband laser ($d = 2.0$ mm, $q_{sat.} = 0.3$) using a split-step Fourier simulation.

3.2 Application in frequency metrology and optical clocks

As previously explained, optical frequency metrology and optical-clock designs require measurements of both degrees of freedom of a femtosecond laser, its repetition rate f_r and its carrier envelope offset frequency f_0. This section briefly discusses how the broadband 1 GHz laser described in the last section is different from (and offers advantages over) the standard 1 GHz laser because of the way that the new laser's offset frequency is measured.

The standard ν-to-2ν-scheme for measuring f_0 is to frequency double a low-frequency portion of the laser spectrum (typically $\approx$1100 nm) and beat it against a spectral matching, high-frequency part of the fundamental spectrum ($\approx$550 nm) [5]. This approach requires a spectrum covering at least one octave. For standard lasers, the only way to attain such a broad spectrum

has been SPM in microstructure fibers. However, coupling light into the core of fibers with a diameter less than 2 μm is a difficult task. As SPM is a third-order nonlinearity, slight changes in coupling efficiency can result in large changes of the attained spectrum and usually limit the time over which a measurement of f_0 can be maintained with sufficient signal-to-noise ratio. Apart from that, microstructure fibers also limit the amount of useful average power achievable for the continuum spectrum because the nonlinear broadening process inherently amplifies both technical and shot noise present on the input light. (References 10 and 27 provide an overview on noise amplification during supercontinuum generation in microstructure fibers.)

The broadband laser allows one to circumvent these problems with microstructure fiber because its broad spectral coverage allows for a direct measurement of its offset frequency. Although the output spectrum has wavelength components that are one octave apart, the power contained in them is too low to facilitate a measurement of f_0 using the standard v-to-$2v$ method. Therefore, we employ a $2v$-to-$3v$ method: A portion around 930 nm is frequency tripled and beat against the second harmonic of a portion around 620 nm to yield a signal at f_0. Details of this setup can be found in Ramond et al. [28].

Although the $2v$-to-$3v$ method is more complicated than the standard method, the broadband laser has an unprecedented long-term stability as a frequency measurement tool. First, it routinely stays mode locked for periods of many days (>1 week demonstrated) without noticeable changes to its output power or spectrum. Second, the f_0 signal usually has a signal-to-noise ratio of 25–30 dB in the 300 kHz bandwidth and does not degrade over time because of the absence of microstructure fiber in the measurement apparatus.

In a test of its long-term stability, we have operated the laser in an optical clock configuration. Here, the repetition rate f_r of the broadband laser is phase locked to a cavity-stabilized single-frequency laser diode at frequency $f_{LD} = 456$ THz that represents the optical frequency standard that would be used in an optical clock. Specifically, a beat between the laser diode and the neighboring component of the frequency comb with frequency f_b has been phase locked to a synthesizer at 600 MHz by feedback to the femtosecond laser's cavity length via a mirror mounted onto a piezoelectric transducer. (All synthesizers were referenced to the NIST primary standard.) Additionally, f_0 was phase locked to a synthesizer at 100 MHz by feedback to the pump power via an acousto-optic modulator. It can be shown that f_r now derives its frequency and instability entirely from the laser diode or, in the case of an optical clock, from the optical frequency standard and is effectively the microwave output of the optical clock [23]. We then counted f_0, f_b and f_r simultaneously with frequency counters at 10 s gate time. The

offset of the counter readings from their preset values ($f_0 = 100$ MHz, $f_b = 600$ MHz, set by the synthesizers; $f_r = 998,092,449.54$ Hz, defined by f_{LD} and the choices of f_0 and f_b) over a period of 21 hours are displayed in Figure 3-10. The data set shows uninterrupted and hands-off operation of the f_0 phase lock for 21 hours with counter-resolution-limited deviations on the millihertz scale until the system was turned off. The phase lock on f_b operated similarly for ≈ 14 h with only one detected feedback-loop error (cycle slip) at ≈ 4 h, i.e., ≈ 10 h of continuously phase-locked data were obtained. The failure at ≈ 14 h was likely caused by the failure of the stabilization of f_{LD} to the Fabry-Perot cavity that prevented the feedback loop from tracking the diode laser frequency rather than failure of the femtosecond laser itself. As f_r represents a measurement of the laser diode frequency ($f_{LD} = f_0 + n_{LD}f_r + f_b$, where n_{LD} is the mode number of the frequency comb component against which f_{LD} is beat), the time record of the offset of f_r from 998,092,449.54 Hz can be multiplied with $n_{LD} = 456,857$ to give a record of the temporal drift of the Fabry-Perot cavity on the right axis of the graph in Figure 3-10. The cycle slip in the f_b feedback loop does not appear in the f_r record because the effect of the 120 mHz excursion in f_b results in an error of 260 nHz in f_r, which is below our measurement limit.

These results show that the broadband laser facilitates a phase-coherent, cycle-slip-free link between an optical oscillator at 456 THz and the 1 GHz laser repetition rate for 10 h. In other words, we have the ability to count 1.6×10^{19} optical cycles at 456 THz without ever losing track of the oscillation. It has also been shown that f_r and f_0 of the broadband laser can be continuously phase locked to a synthesizer for more than 48 hours.

4.   CONCLUSION

Ti:sapphire ring oscillators at 1 GHz repetition rate are currently the best available frequency comb generators for optical frequency metrology. They are compact, have a conveniently large comb spacing, and yield 100 times more power per mode than conventional 100 MHz lasers. Their simple ring-laser architecture employing negative dispersion mirrors for GDD control allows repetition rates between 300 MHz and 3.5 GHz with Ti:sapphire. The concept is extendable to other gain media, as has been demonstrated with Cr:forsterite at 433 MHz repetition rate.
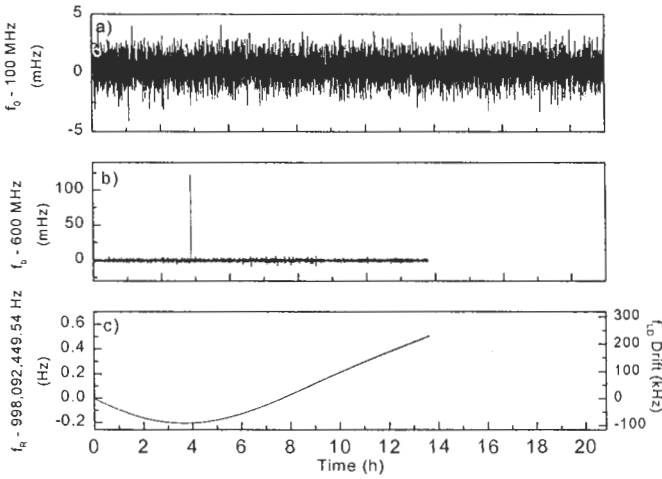
Figure 3-10. (a) A record of consecutive counter readings at 10 s gate time for the phase-locked f_0. The preset value of 100 MHz has been subtracted. (b) The simultaneously measured offset of f_b from 600 MHz. In this plot, one cycle slip of the phase-locked loop controlling f_b has occurred. (c) A time record of the offset of the laser repetition rate from 998,092,449.54 Hz (left scale) that can be translated into a drift of f_{LD} (right scale).

The most critical development has been the 1 GHz broadband Ti:sapphire laser that eliminates troublesome microstructure fibers from optical-frequency-measurement setups. This laser has enabled the construction of an optical clockwork with an unprecedented continuous operation time in excess of 48 hours. This laser might also become interesting in basic research as a source of femtosecond pulses in the range from 620 to 690 nm.

ACKNOWLEDGEMENTS

REFERENCES

[1]   D. E. Spence, P. N. Kean, and W. Sibbett, Opt. Lett. **16**, 42-44 (1991).
[2]   M. Ramaswamypaye and J. G. Fujimoto, Opt. Lett. **19**, 1756-1758 (1994).
[3]   A. Stingl, C. Spielmann, R. Szipocs, and F. Krausz, in *Conference on Lasers and Electrooptics* (Opt. Soc. Am., 1996), p. 66
[4]   T. Udem, J. Reichert, R. Holzwarth, and T. W. Hänsch, Phys. Rev. Lett. **82**, 3568-3571 (1999).
[5]   D. J. Jones, S. A. Diddams, J. K. Ranka, A. Stentz, R. S. Windeler, J. L. Hall, and S. T. Cundiff, Science **288**, 635-639 (2000).
[6]   S. A. Diddams, D. J. Jones, J. Ye, S. T. Cundiff, J. L. Hall, J. K. Ranka, R. S. Windeler, R. Holzwarth, T. Udem, and T. W. Hänsch, Phys. Rev. Lett. **84**, 5102-5105 (2000); M. Niering, R. Holzwarth, J. Reichert, P. Pokasov, T. Udem, M. Weitz, T. W. Hänsch, P. Lemonde, G. Santarelli, M. Abgrall, P. Laurent, C. Salomon, and A. Clairon, Phys. Rev. Lett. **84**, 5496-5499 (2000); S. A. Diddams, T. Udem, J. C. Bergquist, E. A. Curtis, R. E. Drullinger, L. Hollberg, W. M. Itano, W. D. Lee, C. W. Oates, K. R. Vogel, and D. J. Wineland, Science **293**, 825-828 (2001); J. Stenger, T. Binnewies, G. Wilpers, F. Riehle, H. R. Telle, J. K. Ranka, R. S. Windeler, and A. J. Stentz, Phys. Rev. A **63**, 021802 (2001); T. Udem, S. A. Diddams, K. R. Vogel, C. W. Oates, E. A. Curtis, W. D. Lee, W. M. Itano, R. E. Drullinger, J. C. Bergquist, and L. Hollberg, Phys. Rev. Lett. **86**, 4996-4999 (2001); G. D. Rovera, F. Ducos, J. J. Zondy, O. Acef, J. P. Wallerand, J. C. Knight, and P. S. Russell, Meas. Sci. Techn. **13**, 918-922 (2002).
[7]   J. Reichert, R. Holzwarth, T. Udem, and T. W. Hänsch, Opt. Commun. **172**, 59-68 (1999).
[8]   J. K. Ranka, R. S. Windeler, and A. J. Stentz, Opt. Lett. **25**, 25-27 (2000); J. C. Knight, T. A. Birks, P. S. Russell, and D. M. Atkin, Optics Letters **21**, 1547-1549 (1996).
[9]   L. Hollberg, C. W. Oates, E. A. Curtis, E. N. Ivanov, S. A. Diddams, T. Udem, H. G. Robinson, J. C. Bergquist, R. J. Rafac, W. M. Itano, R. E. Drullinger, and D. J. Wineland, IEEE J. Quantum Electron. **37**, 1502-1513 (2001).
[10]   K. L. Corwin, N. R. Newbury, J. M. Dudley, S. Coen, S. A. Diddams, K. Weber, and R. S. Windeler, Phys. Rev. Lett. **90**, 113904 (2003).
[11]   T. Brabec, C. Spielmann, and F. Krausz, Opt. Lett. **17**, 748-750 (1992).
[12]   R. L. Fork, O. E. Martinez, and J. P. Gordon, Opt. Lett. **9**, 150-152 (1984).
[13]   F. Gires and C. R. Tournois, Science **258**, 6112 (1964); R. Szipocs, K. Ferencz, C. Spielmann, and F. Krausz, Opt. Lett. **19**, 201-203 (1994).
[14]   A. Bartels, T. Dekorsy, and H. Kurz, Opt. Lett. **24**, 996-998 (1999).
[15]   H. W. Kogelnik, C. V. Shank, A. Dienes, and E. P. Ippen, IEEE J. Quantum Electron. **8**, 373 (1972).
[16]   A. Bartels, T. Dekorsy, and H. Kurz, in *Conference on Lasers and Electro-Optics* (OSA Technical Digest, 2000), p. CMF3

[17]   A. E. Siegman, *Lasers* (University Science Books, Mill Valley, California, 1986).

[18]   S. A. Diddams, T. Udem, K. R. Vogel, C. W. Oates, E. A. Curtis, R. S. Windeler, A. Bartels, J. C. Bergquist, and L. Hollberg, in *Laser Frequency Stabilization: Standards, Measurement and Applications*, edited by J. L. Hall and J. Ye (SPIE, San Jose, 2001), Vol. SPIE 4269, p. 77-83.

[19]   I. Thomann, A. Bartels, K. L. Corwin, N. R. Newbury, L. Hollberg, S. A. Diddams, J. W. Nicholson, and M. F. Yan, Opt. Lett. **28**, 1368-1370 (2003).

[20]   I. Thomann, L. Hollberg, S. A. Diddams, and R. Equall, Appl. Optics **42**, 1661-1666 (2003).

[21]   J. W. Nicholson, M. F. Yan, P. Wisk, J. Fleming, F. DiMarcello, E. Monberg, A. Yablon, C. Jorgensen, and T. Veng, Opt. Lett. **28**, 643-645 (2003).

[22]   K. L. Corwin, I. Thomann, T. Dennis, R. W. Fox, W. Swann, E. A. Curtis, C. W. Oates, G. Wilpers, A. Bartels, S. L. Gilbert, L. Hollberg, N. R. Newbury, S. A. Diddams, J. W. Nicholson, and M. F. Yan, Opt. Lett. **29**, 397-399 (2004).

[23]   A. Bartels, N. R. Newbury, I. Thomann, L. Hollberg, and S. A. Diddams, Opt. Lett. **29**, 403-405 (2004).

[24]   R. Ell, U. Morgner, F. X. Kärtner, J. G. Fujimoto, E. P. Ippen, V. Scheuer, G. Angelow, T. Tschudi, M. J. Lederer, A. Boiko, and B. Luther-Davies, Opt. Lett. **26**, 373-375 (2001).

[25]   A. Bartels and H. Kurz, Opt. Lett. **27**, 1839-1841 (2002).

[26]   Y. Chen and H. A. Haus, J. Opt. Soc. Am. B **16**, 24-30 (1999).

[27]   N. R. Newbury, B. R. Washburn, K. L. Corwin, and R. S. Windeler, Opt. Lett. **28**, 944-946 (2003).

[28]   T. M. Ramond, S. A. Diddams, L. Hollberg, and A. Bartels, Opt. Lett. **27**, 1842-1844 (2002).